Accurate estimation of the attenuation coefficient from axial point spread function corrected OCT scans of a single layer phantom

Ghafaryasl, Babak, Vermeer, Koenraad, Kalkman, J., Callewaert, Tom, de Boer, Johannes, et al.

Babak Ghafaryasl, Koenraad A. Vermeer, J. Kalkman, Tom Callewaert, Johannes F. de Boer, Lucas J. van Vliet, "Accurate estimation of the attenuation coefficient from axial point spread function corrected OCT scans of a single layer phantom ," Proc. SPIE 10483, Optical Coherence Tomography and Coherence Domain Optical Methods in Biomedicine XXII, 104832B (14 February 2018); doi: 10.1117/12.2292002

SPIE.

Event: SPIE BiOS, 2018, San Francisco, California, United States

Accurate estimation of the attenuation coefficient from axial point spread function corrected OCT scans of a single layer phantom

Babak Ghafaryasl[1,2], Koenraad A. Vermeer[1], J. Kalkman[2], Tom Callewaert[2],

Johannes F. de Boer[3], Lucas J. van Vliet[2].

[1]Rotterdam Ophthalmic Institute, Rotterdam Eye Hospital, Rotterdam, The Netherlands,

[2]Department of Imaging Physics, Delft University of Technology, Delft, The Netherlands,

[3]Department of Physics and Astronomy, Vrije Universiteit Amsterdam, The Netherlands.

ABSTRACT

The attenuation coefficient (AC) is a property related to the microstructure of tissue on a wavelength scale that can be estimated from optical coherence tomography (OCT) data. Since the OCT signal sensitivity is affected by the finite spectrometer/detector resolution called roll-off and the shape of the focused beam in the sample arm, ignoring these effects leads to severely biased estimates of AC. Previously, the signal intensity dependence on these factors has been modeled. In this paper, we study the dependence of the estimated AC on the beam-shape and focus depth experimentally. A method is presented to estimate the axial point spread function model parameters by fitting the OCT signal model for single scattered light to the averaged A-lines of multiple B-scans obtained from a homogeneous single-layer phantom. The estimated model parameters were used to compensate the signal for the axial point spread function and roll-off in order to obtain an accurate estimate of AC. The result shows a significant improvement in the accuracy of the estimation of AC after correcting for the shape of the OCT beam.

Keywords: OCT, attenuation coefficient, focus, Rayleigh length, beam-shape, point spread function, Cramér-Rao lower bound.

INTRODUCTION

The attenuation coefficient (AC) is an optical tissue property that can be estimated from data acquired by optical coherence tomography (OCT). It has potential as a biomarker for the diagnosis and monitoring of diseases, e.g. in chorioretinal disease [1]. Recently, a depth-resolved method was developed to estimate AC coefficient from OCT data [2]. The Fourier-domain OCT signal at a certain depth z in a homogeneous sample whose concentration adheres to the single scattering of light can be written as,

$$I(z) = r(z; w).\frac{Ce^{-2z\mu}}{\left(\frac{z-z_0}{2z_R}\right)^2+1} + \varepsilon(z) \quad (1)$$

Optical Coherence Tomography and Coherence Domain Optical Methods in Biomedicine XXII, edited by Joseph A. Izatt, James G. Fujimoto, Valery V. Tuchin, Proc. of SPIE Vol. 10483, 104832B · © 2018 SPIE · CCC code: 1605-7422/18/$18 · doi: 10.1117/12.2292002

where the first factor, $r(z;w)$, models the so-called roll-off, the depth-dependent signal decay caused by discrete signal detection and resolution limitations of the detection process [3]. The numerator and denominator of the second factor model, respectively, the signal decay as a result of the attenuation coefficient, μ, and the signal dependency caused by the axial point spread function (PSF) [4], where z_0 is the location of the focal point, z_R the Rayleigh length in the medium and *C* a scaling factor. To estimate the AC μ, the OCT signal in Eq. 1 should be corrected for: 1) the noise effect by subtracting the depth-dependent noise floor $\varepsilon(z)$ and removing the noise region [5]; 2) the roll-off by $I(z)/r(z;w)$ after estimating the parameter *w*; and 3) the effect of the axial PSF by multiplication with a factor of $((z-z_0)/2z_R)^2+1$.

We investigated the dependency of the estimated AC on the estimated axial PSF model parameters. The simulated OCT signal of a sample with AC of 3 mm^{-1} while having the focus of the beam located 0.2 mm inside the medium for a system with roll-off parameter $w = 1.7$ and $z_R = 60$ μm is shown in Fig 1a. The sample's AC is calculated from the OCT signal by using the existing method [2] before and after compensation for the effect of axial PSF (Fig 1b). Figure 1c-d shows the estimated AC for several errors in the axial PSF model parameters. Next, Fig 1e-f depict the mean and standard deviation (SD) of the estimated AC within a depth range of 0.5 mm inside the medium for estimation errors in the location of focus and Rayleigh length parameters (relative to the Rayleigh length). As it can be seen, estimation of AC is sensitive to errors in the estimated axial PSF function parameters. Therefore, we need a method to accurately estimate these parameters. In this paper, we will estimate the model parameters by fitting the OCT signal model of Eq. 1 to the measurements obtained from an OCT system, to correct for roll-off and the shape of the focused light to obtain a more accurate estimation of AC. Additionally, *Cramér-Rao* analysis was applied to evaluate the precision of the estimation of the model parameters.

METHOD

We present a method to estimate the axial PSF model parameters by fitting the OCT signal model for single scattered light of Equation 1 to the recorded OCT data obtained from a single layer sample. In addition, Cramér-Rao analysis was applied to estimate the optimal precision of the estimated parameters.

2.1. Estimating the model parameters

To estimate the axial PSF model parameters, the second factor of Eq. 1 was fitted to the measurements corrected for roll-off and noise floor. Let $\boldsymbol{I}(\boldsymbol{Z})$ be a $N_A \times N_z$ matrix of averaged A-lines, with N_A the number of averaged A-lines and N_z the number of data points comprising each A-line. The model parameters C and z_o, common among the A-lines within a B-scan, and μ and z_R, common among the A-lines in all B-scans, can be estimated by minimizing the sum of squared residuals, χ, given by,

$$\chi = \sum_{i=1}^{N_A}\sum_{j=1}^{N_z}\left(\varepsilon_i(z_j)\right)^2 = \sum_{i=1}^{N_A}\sum_{j=1}^{N_z}\left(I_i(z_j) - C_i\frac{e^{-2\,\mu z_j}}{\left(\frac{z_j - z_{o_i}}{2z_R}\right)^2+1}\right)^2. \quad (2)$$

The sequential quadratic programming optimization technique [Curve Fitting Toolbox, MATLAB 2013; The MathWorks, Natick, MA] has been used to estimate the model parameters by solving $\mu, z_R, \{C_i, z_{o_i}\} = \text{argmin}\, \chi$. Boundary conditions were applied based on our knowledge of the system and the sample's optical characteristics.

2.2 Cramér-Rao Lower bound (CRLB)

The precision of the estimated parameters $\Theta = \{\Theta_1, \ldots, \Theta_N\} = \{\mu, z_R, \{C_i, z_{o_i}\}\}$ obtained from the fit to the measurements can be evaluated numerically by calculating the CRLB, which is the inverse of the Fisher information matrix. For a set of independent unknown parameters Θ, the Fisher information matrix for N_z independent measured data-points with additive noise with variance σ^2 and expected values $S(z_j; \Theta)$ can be calculated by [6],

$$\mathbf{F} = \frac{1}{\sigma^2} \sum_{j=1}^{N_z} \frac{\partial S(z_j;\Theta)}{\partial \Theta} \frac{\partial S(z_j;\Theta)}{\partial \Theta^T}. \tag{3}$$

For a set of unbiased estimators of the parameters, the CRLB yields the lower bound on the variance. This implies that the variance of any unbiased estimator of a parameter is higher than or equal to the corresponding diagonal elements of the CRLB matrix [6]. In order to compare the CRLB values, the dimensionless relative CRLB (rCRLB) needs to be calculated by [6],

$$\text{rCRLB}_{ij} = \sqrt{\frac{|\text{CRLB}_{ij}|}{\mu_i \mu_j}}. \tag{4}$$

EXPERIMENTS AND RESULTS

Two B-scans of a thick sample with 0.25 w% of TiO_2 in silicon, located at 0.4 mm from the zero delay line, are recorded with the focal plane set to respectively 0.210 mm and 0.396 mm inside the medium using a Ganymede-II-HR Thorlabs spectral domain OCT system (GAN905HV2-BU). The roll-off parameter *w* was measured to be 1.69, which was used to correct the A-lines for roll-off. The averaged noise floor was obtained by averaging over a large number of A-lines without a sample in the sample arm, and subtracted from each subsequent A-line. Finally, after averaging the A-lines in the B-scan, the noise regions above and inside the sample were removed [5]. Additionally, in the averaged A-lines, the first 0.1 mm inside the medium was affected by specular reflection and therefore excluded from all subsequent processing steps.

Before analyzing the measured OCT data, we simulated two OCT signals where the parameters were set to $C = 2.5 \cdot 10^4$, μ = 3 mm^{-1}, z_R = 0.56 mm, and the location of the focus was set to respectively z_0 = 0.21 mm and 0.396 mm inside

the sample. In Figure 2, the rCRLB values of the simulated OCT signals were calculated from Equations 3 and 4 where σ^2 was considered to be 300 and constant for all the depths.

Then, in the measured data, the OCT signal model was fitted to the processed A-lines where the model parameters μ and z_R were considered to be common among the B-scans, and z_o and C were estimated individually for each B-scan. The initial value of μ was set to 3.1 mm^{-1}, z_R to 52 μm, C to $5 \cdot 10^3$ for both B-scans, and z_o to 0.3 mm for both B-scans. For z_R, μ, and z_o the lower bound on the parameters was set to 40 um, 1 mm^{-1} and -1.2 mm; and the upper bound to 90 um, 4 mm^{-1} and 1.2 mm, respectively. The result of the best fit to the measurements is shown in Figure 3a. The estimated values of the common parameters were μ = 2.8 mm^{-1} and $z_R = 63$ μm. The locations of focus were estimated to be 0.208 mm for the first and 0.391 mm for the second B-scan. The AC was estimated using the depth-resolved method [2] before and after correcting for the axial PSF of the OCT beam with the estimated parameters (Figure 3b). A significant improvement of the estimated AC can be seen in Figure 3b after correcting for the axial PSF, especially within 0.3 mm inside the sample. For two measurements with different locations of focus, the mean and SD of the AC, after correcting for the shape of the OCT beam, were calculated for different depths ranging from 0.1 mm to a certain depth inside the sample, and the results are shown in Figures 3c-d.

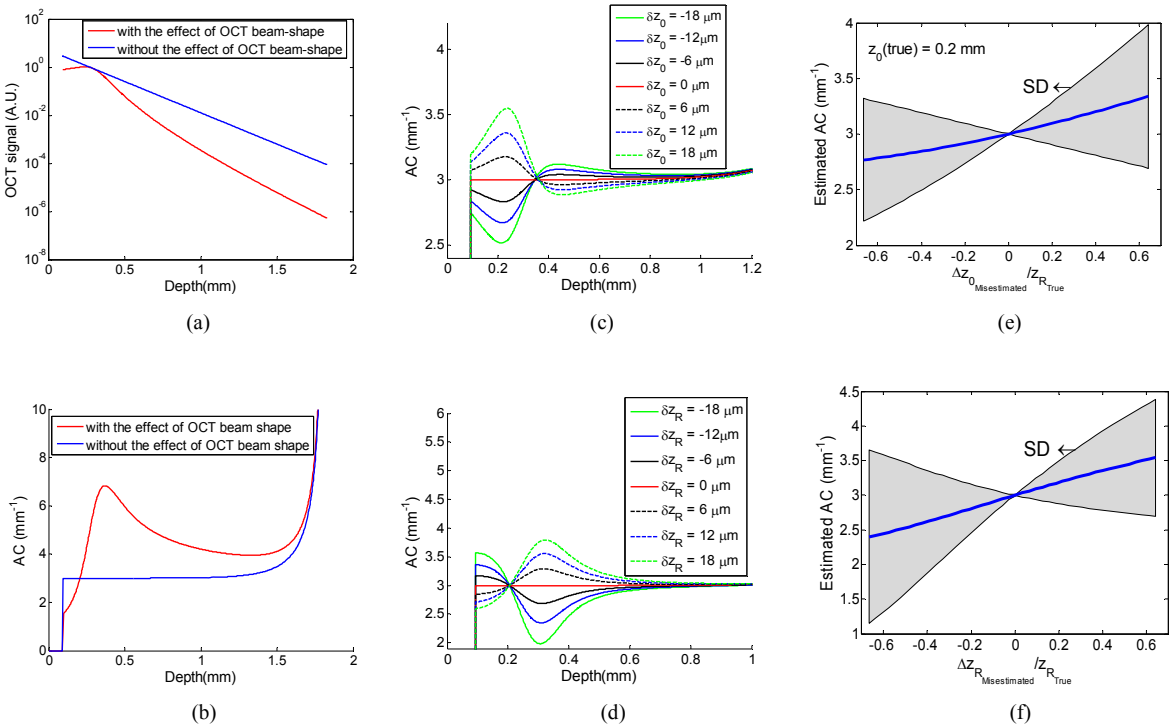

Figure 1. Simulated OCT signal (a) and estimated AC (b) with and without the effect of the OCT beam-shape; Estimated AC for several errors in: c) the focus location; and d) Rayleigh length. The average and SD of AC over a depth range of 0.5 mm inside the medium for the relative estimation errors between $[-0.066, 0.066]$ in e) the location of focus and f) Rayleigh length.

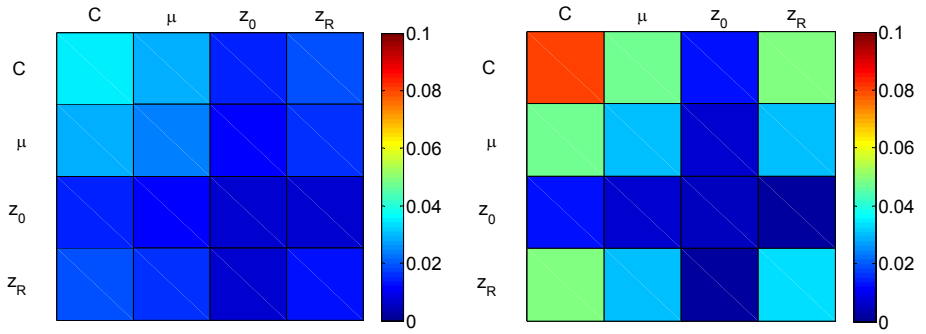

Figure 2. The rCRLB matrix values of the model at two locations of the focal point i.e. 0.21 mm (left) and 0.396 mm (right).

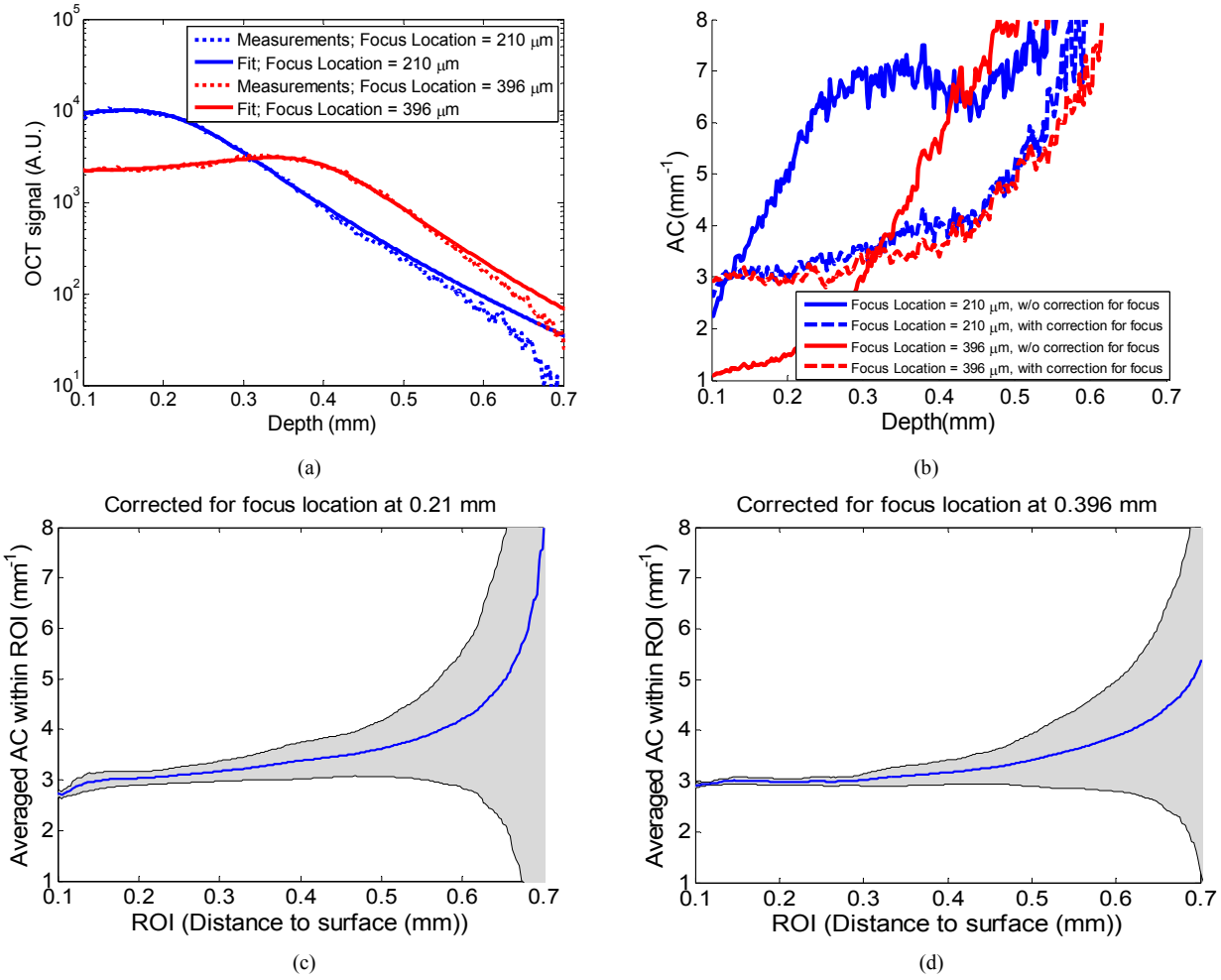

Figure 3. a) The measured OCT signals and the best-fitted model for a focus location at 0.21 mm and 0.39 mm inside the medium. b) Estimated ACs before and after correcting for the shape of OCT beam with the estimated parameters for two measurements. The mean and SD of AC for the varying region of interest (ROI) = $[0.1, z_{depth}]$ mm, for measurements with the location of focus at c) 0.21 mm and, d) 0.396 mm inside the medium.

CONCLUSION

In this paper, we present a method to improve the accuracy of estimating the attenuation coefficient by compensating for the shape and focus position of the OCT beam. The axial PSF model parameters were also estimated from the recorded OCT data. Cramér-Rao analysis was used to obtain the optimal precision of the parameter estimation with the proposed method. The rCRLB results show that for the locations of the focus investigated in this work the minimum variance of the estimated parameters were below 10% which is acceptable. The experimental results in Figure 3.b show a significant improvement in the estimated AC, especially within [0.1, 0.3] mm inside the sample. From the results of Cramér-Rao analysis in Figure 2, we expect a lower variation in the estimation of AC for the focus located at 0.21 mm inside the sample compared to the location of focus at 0.396 mm. However, the results in Figure 3 c-d show smaller variation of the ACs with the focus located at 0.396 mm. This could be due to the misestimating the roll-off, depth-dependent noise floor, etc. and requires further investigation.

ACKNOWLEDGMENT

This research was partially funded by the Netherlands Organization for Health Research and Development (ZonMw) TOP grant (91212061). We would like to acknowledge Dr. Dirk H. J. Poot[1] for his technical support in this work.

REFERENCES

[1] K.A. Vermeer, J. van der Schoot, H.G. Lemij, and J.F. de Boer, "RPE-normalized RNFL attenuation coefficient maps derived from volumetric OCT imaging for glaucoma assessment," Investigative Ophthalmology & Visual Science, Vol. 53, pp. 6102-6108, 2012.

[2] K.A. Vermeer, J. Mo, J.J. Weda, H.G. Lemij, and J.F. de Boer, " Depth-resolved model-based reconstruction of attenuation coefficients in optical coherence tomography," Biomedical Optics Express, Vol. 5, pp. 322-337, 2013.

[3] S.H. Yun, G.J. Tearney, B.E. Bouma, B.H. Park, and J.F. de Boer, "High-speed spectral-domain optical coherence tomography at 1.3 μm wavelength," Optics Express, Vol. 11, pp. 3598-3604, 2003.

[4] T.G. van Leeuwen, D.J. Faber, and M.C. Aalders, "Measurement of the axial point spread function in scattering media using single-mode fiber-based optical coherence tomography," IEEE J. Sel. Top. Quantum Electronics, Vol. 9, pp. 227-233, 2003.

[5] B. Ghafaryasl, K.A. Vermeer, J.F. de Boer, M.E.J. van Velthoven, L.J. van Vliet, "Noise-adaptive attenuation coefficient estimation in spectral domain optical coherence tomography data." IEEE 13th International Symposium of Biomedical Imaging (ISBI), pp 706-709, 2016.

[6] M.W.A. Caan, H.G. Khedoe, D.H.J. Poot, A.J. den Dekker, S.D. Olabarriaga, K.A. Grimbergen, L.J. van Vliet, F.M. Vos. "Estimation of Diffusion Properties in Crossing Fiber Bundles." IEEE Transactions on Medical Imaging, Vol. 29, No. 8, pp. 1504-515, 2010.

[1] Biomedical Imaging Group Rotterdam, departments of Medical Informatics and Radiology, Erasmus Medical Center Rotterdam, Rotterdam, The Netherlands